GA–A26757

SOL WIDTH AND TRANSPORT IN LIMITED VERSUS DIVERTED DISCHARGES IN DIII-D

by
D.L. RUDAKOV, J.A. BOEDO, R.A. PITTS, G.L. JACKSON,
C.J. LASNIER, A.W. LEONARD, R.A. MOYER, P.C. STANGEBY,
G.R. TYNAN, and J.G. WATKINS

JULY 2010

GENERAL ATOMICS

DISCLAIMER

GA– A26757

SOL WIDTH AND TRANSPORT IN LIMITED VERSUS DIVERTED DISCHARGES IN DIII-D

by
D.L. RUDAKOV,* J.A. BOEDO,* R.A. PITTS,† G.L. JACKSON,
C.J. LASNIER,‡ A.W. LEONARD, R.A. MOYER,* P.C. STANGEBY,¶
G.R. TYNAN,* and J.G. WATKINS§

This is a preprint of a paper to be presented at the Nineteenth International Conference on Plasma Surface Interactions, May 24-28, 2010, in San Diego, California, and to be published in the *Proceedings.*

* University of California-San Diego, La Jolla, California.
† ITER Organization, St. Paul-lez-Durance Cedex, France
‡ Lawrence Livermore National Laboratory, Livermore, California.
¶ University of Toronto Institute for Aerospace Studies, Toronto, Canada.
§ Sandia National Laboratories, Albuquerque, New Mexico.

Work supported by
the U.S. Department of Energy
under DE-FC02-04ER54698, DE-FG02-07ER54917,
DE-AC52-07NA27344, and DE-AC04-94AL85000

GENERAL ATOMICS ATOMICS PROJECT 30200
JULY 2010

GENERAL ATOMICS

ABSTRACT

An experiment aimed at benchmarking the ITER scrape-off layer (SOL) power width scaling in limited L-mode discharges has been conducted on DIII-D. Scans of the main scaling parameters were performed in an inner-wall-limited (IWL) magnetic configuration. Using the near-SOL density and temperature e-folding lengths, λ_n, λ_T, determined from reciprocating Langmuir probe measurements, SOL power flux density e-folding lengths, λ_q, are derived. A few lower single null (LSN) discharges were also run for comparison. The results are generally in agreement with the ITER design assumptions, finding that λ_n and λ_T are correlated $\left(\lambda_T \sim 1.2\,\lambda_n\right)$ and both λ_n and λ_T are on average 2.1-2.5 times larger in IWL configurations than in LSN. In moderate elongation $\left(\kappa \sim 1.4\right)$ IWL discharges, λ_q is largest and agrees with the assumed ITER scaling within the estimated uncertainty (a factor of ~ 2). In IWL discharges λ_q measurements are consistent with the expectations of SOL power balance.

I. INTRODUCTION

Plasma facing components (PFCs) in ITER will have to withstand much higher incident fluences of particles and energy than those encountered in present day tokamaks [1]. Like many tokamaks, plasma start-up and ramp-down in ITER will use limiter configurations, with the majority of the discharge time spent in diverted lower single null (LSN) magnetic configuration. The ITER first wall (FW) is being designed to allow startup on the actively cooled beryllium panels on both the high (HFS) and low (LFS) field sides, and plasma scenarios have been developed [2]. During start-up, they are designed to minimize the time spent in limiter configuration both to assist in reducing power loading and reduce flux consumption during the plasma current $\left(I_p\right)$ ramp. Transitions to LSN are expected around t = 13 s at $I_p \sim 3.5$ MA. During the ramp down phases, plasma elongation, density and current will all have to be reduced in a controlled way to avoid too much contact with the outer wall at high power. Current scenarios have limiter contact only at the very end of the ramp-down when $I_p \sim 1.5$ MA [2].

Power handling is determined by the parallel heat flux density, $q_{||}$ and the panel shaping. The former is characterized by the SOL power flux density e-folding length, λ_q. In the ITER Thermal Load Specifications [2,3] which form the design basis for the FW and divertor PFCs, λ_q in L-mode divertor phases is estimated assuming the scaling derived from measurements of divertor target power fluxes mostly from JT-60U and JET (with an uncertainty of a factor of ~ 2 around this value):

$$\lambda_q(\mathrm{m}) = (1 \pm 1/3)\, 3.6\ 10^{-4}\ \mathrm{R\ (m)}^2\ P_{div}\,(\mathrm{MW})^{-0.8}\ q_{95}^{0.5}\ \bar{n}_e \left(10^{19}\ \mathrm{m}^{-3}\right)^{0.9}\ Z_{eff}^{0.6} \quad , (1)$$

where R is the major radius, P_{div} is the conducted power to the divertor, $\bar{n}_\mathrm{e}$ is the line averaged plasma density and Z_{eff} is the plasma effective charge. In the absence of a similar scaling for limiter plasmas, Eq. (1) has been applied to estimate λ_q for the limiter ramp-up/down phases in ITER by replacing P_{div} by the power to the limiters and taking into account the effect of a variable number of poloidal limiters following the model in Ref. [4].

Experimental measurements in tokamaks show considerably larger SOL width in HFS- compared to LFS-limited configurations (see [5] and references therein). This is explained by the strong ballooning component of edge transport in tokamaks, which leads to larger SOL widths when plasmas are limited on the HFS. A considerable part of this ballooning transport is due to radially propagating plasma filaments (also called “blobs” [6]) with density and temperature above those of the background SOL plasma (see [7]

and references therein). As a consequence, the value of λ_q mapped to the outboard midplane is expected to be $\sim 2.5\times$ higher in HFS limiter plasmas than in their LFS counterparts [4]. When flux expansion is taken into account, the local value of λ_q at HFS in ITER will be $\sim 4\times$ higher than that on the LFS [3]. For given power into the SOL (P_{SOL}), this increase over-compensates the increased parallel power flux (due to the stronger toroidal field on the HFS) and makes HFS start-up advantageous compared with LFS configurations. There are in fact other advantages to HFS start-up [2], so it is important to confirm that these ITER assumptions for limiter power loading are correct. This is even more important in the light of the fact that ITER FW shaping design is in the final stages. Here we report results of the recent λ_q measurements in the DIII-D tokamak performed in inner-wall-limited (IWL) plasmas of varying elongation as well as LSN diverted discharges. A single discharge with the plasma limited at the top of the vessel was acquired as an approximation to LFS-limited conditions, for which the DIII-D FW is not optimized.

II. EXPERIMENTAL ARRANGEMENT

A poloidal cross-section of DIII-D together with the shapes of the last closed flux surface (LCFS) in a few configurations used in this study are shown in Fig. 1. Figure 1(a) shows two IWL configurations with slightly different elongation, $\kappa \sim 1.4$ and $\kappa \sim 1.5$. It is worth noting that δ, the distance between the top of the LCFS and the toroidally continuous surface of the upper outer divertor baffle (known as the "knee limiter") decreases with the increasing elongation. Figure 1(b) shows separatrix in LSN and the LCFS of top-limited (TL) discharges. Also shown are the poloidal location of the midplane reciprocating probe array (RCP) [8] and the field of view of the infrared camera (IRTV). The RCP is used to determine the e-folding lengths, λ_n and λ_T of n_e and T_e in the LFS SOL. Assuming $T_i = T_e$ (since T_i measurements are unavailable) and sheath-limited heat flux, $q \propto n_e T_e^{3/2}$ allows λ_q to be computed according to:

$$\frac{1}{\lambda_q} = \frac{1}{\lambda_n} + \frac{3}{2\lambda_T} \quad . \tag{2}$$

The IRTV measures the heat flux profile across the lower divertor floor and is used to benchmark the probe measurements of λ_q in the LSN configuration.

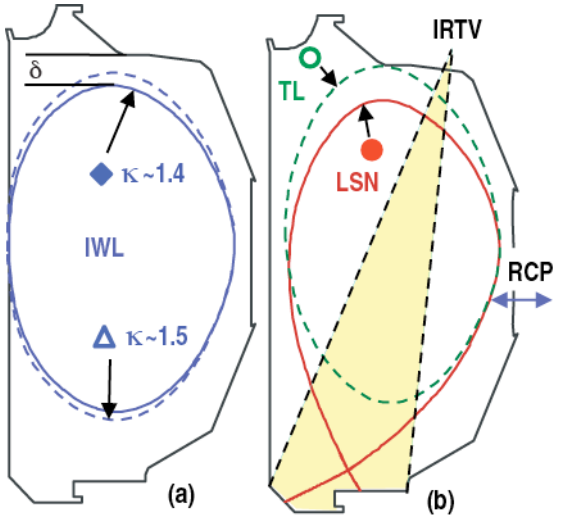

Fig. 1. Poloidal cross-sections of the LCFS in the magnetic configurations used in the study (a,b) and diagnostic arrangement (b). Symbols attached to the LCFS are used in the Figs. 3 – 6 for the corresponding configurations.

III. EXPERIMENTAL RESULTS

The experiment comprised a series of Ohmic and neutral beam injection (NBI) heated L-mode discharges. Profiles of n_e and T_e were measured with the RCP twice per discharge, at t = 2.5 s and t = 3.5 s. Plasma current and density were changed from shot to shot, while NBI heating power, P_{NBI}, was increased stepwise in some of the discharges from 0 to 1.25 MW at t = 3.0 s. The scaling parameters in Eq. (1) were varied in the following ranges: q_{95} = 3.2–7.4, $\overline{n}_{\mathrm{e}} = 1.1\text{–}4.5\times10^{19}$ m^{-3}, $P_{\mathrm{SOL}} = 0.1\text{–}1.4$ MW. Here P_{SOL} is used in place of P_{div} in Eq. (1) and is calculated as the sum of Ohmic and NBI heating power minus the power radiated from the plasma core. There was no systematic change in core impurity concentration throughout the scans with $Z_{eff} \sim 2$ in all discharges. We should note that the scaling parameters were not changing independently. For example, an increase in the heating power typically resulted in an increase in the plasma density.

The full data set consists of 37 IWL, 10 LSN and 2 TL profiles. As discussed later, some of the discharges became detached and should be excluded from comparison with the expectations of Eq. (1). A few profiles were discarded because the probe reciprocations did not allow close enough approach to the LCFS and/or due to excessive scatter in the raw data, resulting in poor fits. Figure 2 shows profiles of n_e and T_e in IWL and LSN discharges with comparable parameters: (a) IWL, I_p = 0.88 MA, $\overline{n}_{\mathrm{e}} = 2.37\times10^{19}$ m^{-3}, P_{SOL} = 0.4 MW; (b) LSN, I_p = 0.88 MA, $\overline{n}_{\mathrm{e}} = 1.76\times10^{19}$ m^{-3}, P_{SOL} = 0.23 MW. The profiles have distinctively different e-folding lengths in "near" (close to the LCFS) and "far" SOL. For the purpose of this study we will focus only on the "near" SOL e-folding lengths.

Figure 3 plots λ_T versus λ_n for all useable profiles in the dataset. There is a good correlation, with $\lambda_T \sim 1.2\,\lambda_n$ on average (dashed line). The large open symbols show averages for IWL (diamond) and LSN (circle) configurations, demonstrating that in the IWL configuration, both λ_T and λ_n are larger than in LSN by factors of 2.54 and 2.13, respectively. Values of λ_q derived from the data of Fig. 3 using Eq. (2) are on the average ~2.4 times larger in IWL than in LSN, directly confirming the ITER assumption. The two available TL profiles have λ_T and λ_n comparable to LSN values (somewhat smaller than the LSN average), also confirming the ITER assumptions.

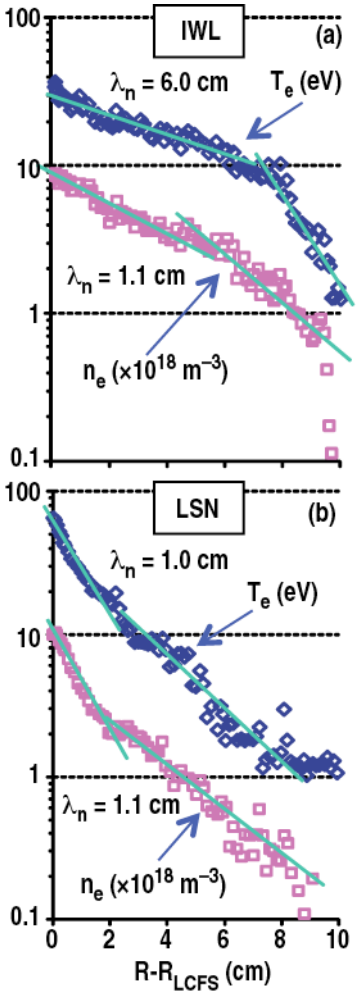

Fig. 2. Typical profiles of n_e and T_e in IWL (a) and LSN (b) discharges.

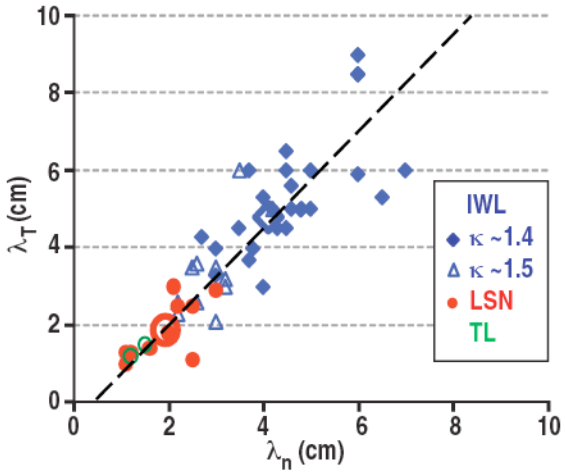

Fig. 3. Correlation between density and temperature e-folding lengths.

A comparison of the λ_q values derived from probe data with those calculated using the scaling in Eq. (1) is shown in Fig. 4(a) for the entire dataset. Based on the results of Fig. 3, the IWL data have been scaled down by a factor of 2.5 to be comparable with LSN data and the scaling assumptions. It is evident from this comparison that our results do not confirm the assumed ITER λ_q scaling. Moreover, the measured values generally tend to be below those given by the scaling. However, the overall disagreement in absolute values is not very large. Figure 4(b) illustrates the I_p dependence of the ratio of measured/scaling λ_q. Whilst all points above unity for this ratio agree with the scaling within a factor of 2, agreement is worse on the lower side. However, Eq. (1) assumes attached conditions, while some of the higher density and lower I_p (higher q_{95}) discharges may have been detached. We do not have a good indication for detachment in IWL discharges, but those which are radiation-dominated, with $P_{\mathrm{SOL}} < 0.25$ MW are likely to be detached. This includes most points circled with a dashed line in Fig. 4. If those points are removed, all remaining lower elongation IWL, TL, and most of LSN measured λ_q values agree with the scaling within a factor of 2, i.e. within the assumed scaling uncertainty. Higher elongation IWL values tend to disagree with the scaling by a larger factor, being up to 4 times smaller even at $I_p \sim 1.2$ MA. This may be due to the closer proximity of the "knee limiter" at the top of the vessel to the LCFS in those discharges. Figure 5 plots the measured λ_q values versus δ, the distance from the LCFS to "knee limiter" (Fig. 1) mapped to midplane, in IWL and TL discharges. The large open symbols denote average values for higher and lower elongation IWL configurations. There is a clear correlation between λ_q and δ, with λ_q in higher κ, lower δ discharges being on the average ~30% lower than in lower κ, higher δ cases. We therefore conclude that the proximity of the secondary limiter to the LCFS may affect the SOL width in higher κ discharges and that data from those discharges may be not suitable for comparison with the scaling of Eq. (1). Removing higher κ points (open triangles) from Fig. 4 would improve agreement of the measured λ_q values with the scaling [Fig. 4(b)], but would still not bring the data into line with the scaling.

In order to check the validity of Eq. (2) for the derivation of λ_q from the probe data, IRTV was used in LSN discharges to benchmark the probe results. Out of 10 LSN profiles, 4 were obtained with the outer strike point (OSP) detached, and IRTV data could not be used. Five out of the remaining six profiles show agreement to within a factor of 2 between λ_q values from IRTV (mapped to the LFS midplane) and the probe, which is reasonable within the measurement uncertainties.

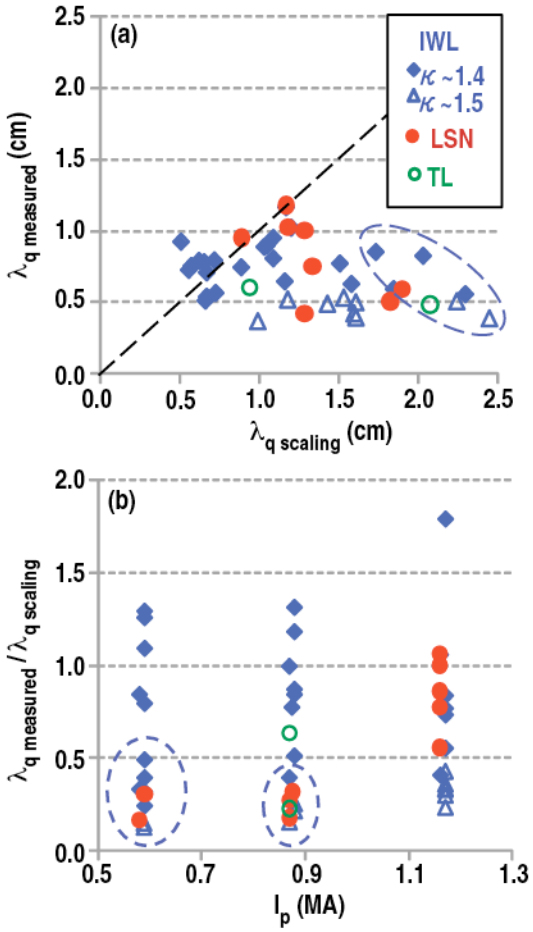

Fig. 4. Comparison of the measured heat flux e-folding length with assumed ITER scaling of Eq. (1). Note that measured IWL values are scaled down by a factor of 2.5.

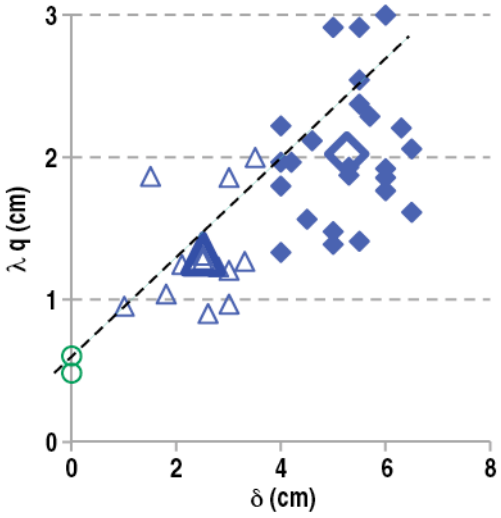

Fig. 5. Dependence of the measured heat flux e-folding length on the distance from the LCFS to "knee limiter" in IWL configuration.

Following the arguments in [5], we can check interdependence between $q_{||}$ and λ_q at the LCFS. Simple SOL power balance [4] yields

$$q_{\mathrm{LCFS}} = \frac{P_{SOL}}{A_{q||}^{SOL}} = \frac{P_{SOL}}{4\pi R\lambda_q (B_\theta / B_\phi)} \propto \frac{P_{SOL} q_{95}}{a\lambda_q} \quad , \tag{3}$$

where a is the minor radius. Figure 6 shows a plot of q_{LCFS} $\left(\propto n_{\mathrm{e,LCFS}} T_{e,LCFS}^{3/2}\right)$ in $\mathrm{MW/m^2}$ versus $P_{SOL} q_{95} / (a\lambda_q)$ for IWL discharges. Most of the data indeed lay close to a linear dependence.

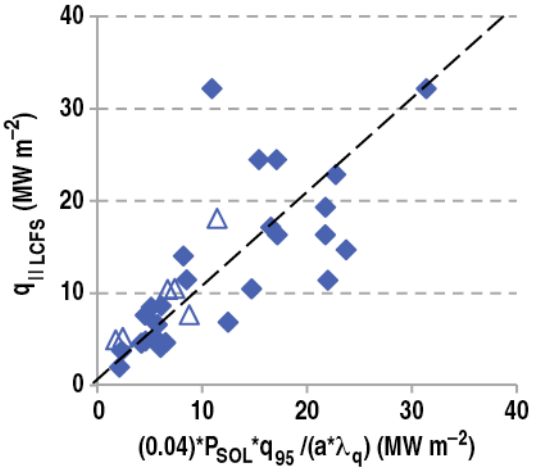

Fig. 6. Comparison of the heat flux at the LCFS derived from the probe data with a simple physics model.

IV. DISCUSSION AND SUMMARY

The primary goals of the DIII-D experiments reported here were to benchmark the ITER SOL power width scaling of Eq. (1) in both limited and diverted configurations and demonstrate the larger power scrape-off width for HFS versus LFS limiter configurations. Three of five scaling parameters (q_{95}, $\overline{n}_e$ and P_{SOL}) were varied in a rather wide range, although they do not vary independently and it is thus impossible with this dataset to check the individual scaling dependencies of Eq. (1). Moreover, the measured λ_q show no correlation with the scaling trends as the plasma parameters change. On the other hand, with the exception of detached discharges and those affected by a proximity of the secondary limiter, the absolute measured values of λ_q agree with the scaling within the assumed uncertainty of a factor of 2. This result lends confidence to the scaling relationship.

We have shown that the SOL power width measured at the outboard midplane in IWL configuration is on average ~2.4 times larger than in LSN, confirming the assumptions used by ITER. We have also confirmed that the parallel heat flux at the LCFS in IWL configuration scales with a physics-based combination of discharge parameters including P_{SOL} and λ_q. Our results were obtained in ITER-relevant elongated plasmas with toroidally continuous limiting surfaces.

The strongest dependence of the scaling in Eq. (1) — the one on the major radius — could not be directly tested in our experiments. However, the fact that our results are in reasonable agreement with a scaling based on data from JT-60U and JET, machines with a considerably larger R, constitutes an approximate confirmation of the validity of the R^2 dependence in Eq. (1). This is an important result, greatly increasing the confidence in applying Eq. (1) to ITER.

REFERENCES

[1] G. Federici, *et al.*, Nucl. Fusion **41** (2001) 1967.

[2] R. A. Pitts *et al.*, these proceedings.

[3] A. Loarte, *et al.,* Proc. 22nd IAEA Fusion Energy Conf., Geneva, Switzerland (2008), Paper IT/P6-13, http://www-pub.iaea.org/MTCD/Meetings/fec2008pp.asp

[4] P.C. Stangeby Nucl. Fusion **50** (2010) 035013.

[5] M. Kocan and J.P. Gunn, Plasma Phys. Control. Fusion **52** (2010) 045010.

[6] S.I. Krasheninnikov, Phys. Lett. A **283** (2001) 368.

[7] D.L. Rudakov *et al.*, Nucl. Fusion **45** (2005) 1589.

[8] J.G. Watkins *et al.,* Rev. Sci. Instrum. **63** (1992) 4728.

ACKNOWLEDGMENT

This work was supported in part by the U.S. Department of Energy under DE-FG02-07ER54917, DE-FC02-04ER54698, DE-AC52-07NA27344, and DE-AC04-94AL85000.